Unlocking the Potential of Battery Research

A New Expert Insight.
Download for free.

Battery research is essential to meet the growing demand for reliable, efficient, cost-effective energy storage solutions.

This expert insight presents recent research on solid polymer electrolytes (SPEs), recycling methods for lithium-ion batteries (LIBs), and cathode degradation during extreme fast charging (XFC) of electric vehicles.

PerkinElmer®
For the Better

WILEY

International Journal of Energy Research

INTERNATIONAL JOURNAL OF ENERGY RESEARCH
Int. J. Energy Res. 2014; **38**:1391–1402
Published online 13 January 2014 in Wiley Online Library (wileyonlinelibrary.com). DOI: 10.1002/er.3148

Process simulation and analysis of a five-step copper–chlorine thermochemical water decomposition cycle for sustainable hydrogen production

Mehmet F. Orhan[1,*,†], Ibrahim Dincer[2] and Marc A. Rosen[2]

[1]Department of Mechanical Engineering, College of Engineering, American University of Sharjah, PO Box: 26666, Sharjah, United Arab Emirates
[2]Faculty of Engineering and Applied Science, University of Ontario Institute of Technology, 2000 Simcoe Street North, Oshawa, Ontario, L1H 7K4, Canada

SUMMARY

A process model of a five-step copper–chlorine (Cu–Cl) cycle is developed and simulated with the Aspen Plus simulation code. Energy and mass balances, stream flows and properties, heat exchanger duties, and shaft work are determined. The primary reactions of the five-step Cu–Cl cycle are assessed in terms of varying operating and design parameters. A sensitivity analysis is performed to examine the effect of parameter variations on other variables, in part to assist optimization efforts. For each cycle step, reaction heat variations with such parameters as process temperature are described quantitatively. The energy efficiency of the five-step Cu–Cl thermochemical cycle is found to be 44% on the basis of the lower heating value of hydrogen, and a parametric study of potential efficiency improvement measures is presented. Copyright © 2014 John Wiley & Sons, Ltd.

KEY WORDS

hydrogen production; thermochemical water decomposition; copper–chlorine cycle; nuclear heat utilization; process simulation; optimization

Correspondence

*Mehmet F. Orhan, Department of Mechanical Engineering, College of Engineering, American University of Sharjah, PO Box: 26666, Sharjah, United Arab Emirates.
†E-mail: morhan@aus.edu

Received 24 September 2013; Revised 6 November 2013; Accepted 20 November 2013

1. INTRODUCTION

Increasing global population and living standards are diminishing supplies of conventional energy resources. Inefficient energy consumption trends tend to further increase energy demand. Fossil fuel use is generally agreed to significantly impact on the environment, particularly the climate, and thus to threaten humanity. These concerns have fostered extensive research into alternative and clean energy technologies and sources. Many natural energy sources (e.g., wind, geothermal, and solar) can be challenging to utilize because of their issues such as energy quality and density. Nuclear energy contributes little to climate change yet can provide an energy supply on a large scale.

Several methods are presented in the literature to produce emission-free hydrogen from nuclear energy. The main candidates are thermochemical cycles and electrolysis of water. The thermochemical production of hydrogen involves a series of chemical reactions, wherein the net result is the combination of heat and water to yield hydrogen and oxygen. The main incentives for thermochemical hydrogen production are potentially higher efficiencies and potential economic advantages of scaling, which may be significantly better than those for electrolysis of water with electricity. The cost of nuclear-based thermochemical hydrogen production is lower than that of nuclear hydrogen production by the electrolysis of water, which could be as low as 60% based on the electricity price. Also, producing hydrogen directly from thermal heat via thermochemical cycles eliminates efficiency losses to convert heat to electricity that is used in the electrolysis of water to produce hydrogen. Therefore, hydrogen production using thermochemical water decomposition is believed by various researchers to provide a beneficial opportunity for large-scale direct use of thermal energy from nuclear plants.

Thermochemical water decomposition based on the copper–chlorine (Cu–Cl) cycle involves a series of chemical reactions that ultimately decompose water into its constituents. The process uses copper and chlorine compounds, but the net inputs are water and heat (with some electricity) and the net outputs oxygen and hydrogen.

Although an apparatus for a complete process has not yet been constructed, numerous studies of the Cu–Cl cycle have been published. Lewis *et al*. [1,2] indicated the Cu–Cl cycle to be viable in terms of engineering and efficiency. A conceptual process design estimates the production cost at $3.30 per kg hydrogen [2]. Recent Canadian advances in nuclear-based hydrogen production via the Cu–Cl cycle have been reported, covering such factors as individual processes and reactors thermochemical properties, materials, controls, safety, reliability, economics, and integration of hydrogen production with Canada's nuclear plants [3]. The design and reliability of control systems for Cu–Cl thermochemical hydrogen production have been investigated [4]. A thermodynamic equilibrium analysis of the Cu–Cl cycle steps has been reported [5]. Solid particle decomposition and hydrolysis reaction kinetics in Cu–Cl have recently been described [6], whereas the solid conversion process during hydrolysis and the decomposition of cupric chloride have been analyzed [7]. Thermophysical properties of copper compounds in the cycle [8] and the kinetics of the copper/hydrochloric acid reaction [9] have been examined.

Equipment scale-up studies and process simulation (using Aspen Plus) have identified the challenges and the design issues of hydrogen production via the Cu–Cl cycle [10]. The overall heat required to produce hydrogen with the cycle was shown to be 543.7 kJ/mol and the energy efficiency 53%.

Design challenges involving reactor scale-up of the Cu–Cl cycle have been examined [11], focusing hydrolysis, hydrogen, and oxygen reactors. Scale-up design issues associated with the molten salt reactor have been described, especially handling the three phase material (including copper oxychloride solid particles, molten salt, and oxygen), whereas differences in the hydrolysis reactor for two, three, and five-step Cu–Cl cycles have been investigated. Heat recovery from molten CuCl has been examined [12], including a counter-current spray flow heat exchanger involving molten CuCl droplets and air. A challenge in the Cu–Cl cycle is the hydrolysis of $CuCl_2$ into $CuO \cdot CuCl_2$ and HCl while avoiding excess water needs and the undesired thermolysis reaction (which yields CuCl and Cl_2). A spray reactor was designed in which an aqueous solution of $CuCl_2$ is atomized into a heated zone, where steam and argon are injected in co-current or counter-current flow [13], while a spray reactor with an ultrasonic atomizer has been studied experimentally [14]. Ceramic carbon electrode materials have been prepared using 3-aminopropyl trimethoxysilane and investigated. At the same time, ceramic carbon electrode-based anodes have been studied to ascertain their potential for use in the Cu–Cl cycle [15,16].

Wang *et al*. [17] have compared sulfur-iodine and copper–chlorine thermochemical hydrogen production cycles in terms of heat quantity and grade, efficiency, engineering viability, and cost. Preliminary studies of the Cu–Cl cycle and small lab scale experiments for cycle reactions have been performed. Yet to improve understanding and facilitate commercialization, a need exists to join the cycle steps and construct a pilot plant. Experimental studies of the overall cycle are necessary, including energy, exergy, and cost studies. Simulation with tools such as Aspen Plus need to be employed to provide the design, optimization, and operation information required to build a pilot plant.

This study aims to analyze the five-step Cu–Cl cycle and develop simulations with Aspen Plus, while utilizing experimental results obtained by University of Ontario Institute of Technology, Argonne National Laboratory, Atomic Energy of Canada Limited, and others. Energy and mass balances, stream flows and properties, heat exchanger duties, and shaft work are determined. The primary reactions of the five-step Cu–Cl cycle are assessed in terms of varying operating and design parameters. A sensitivity analysis is performed to examine the effect of parameter variations on other variables, in part to assist optimization efforts. For each cycle step, reaction heat variations with such parameters as process temperature are described quantitatively. A parametric study of potential efficiency improvement measures is presented.

2. SYSTEM STUDIED

In the five-step Cu–Cl cycle (Figure 1), water and nuclear-derived heat are input, and H_2 and O_2 are produced. The five steps, which include three thermochemical reactions and one electrochemical reaction, follow:

1. hydrolysis,
2. oxy-decomposition,
3. electrolysis,
4. drying, and
5. hydrogen production.

All steps involve chemical reactions except drying. The liquid water entering the cycle is at ambient temperature and passes through several heat exchangers where it evaporates and is heated to 400°C using heat from cooling the hydrogen and oxygen gases before they exit the cycle. Note that all temperatures used in this section are values at the normal operating conditions and may change during the sensitivity analyses. Steam and solid copper chloride ($CuCl_2$) from the dryer, both at 400°C, enter the fluidized bed (S1), where the following chemical reaction (hydrolysis) occurs:

$$2CuCl_2(s) + H_2O(g) \rightarrow CuO{\cdot}CuCl_2(s) + 2HCl(g) \quad (1)$$

This reaction is endothermic and yields hydrochloric acid gas (HCl), which is compressed, and $CuO \cdot CuCl_2$, which is transferred to another process step after it is heated to the oxy-decomposition (oxygen production) reaction temperature of 500°C.

In the oxy-decomposition step (S2), $CuO \cdot CuCl_2$ is heated, and O_2 and copper monochloride (CuCl) are produced via the following endothermic chemical reaction:

Int. J. Energy Res. 2014; **38**:1391–1402 © 2014 John Wiley & Sons, Ltd.
DOI: 10.1002/er

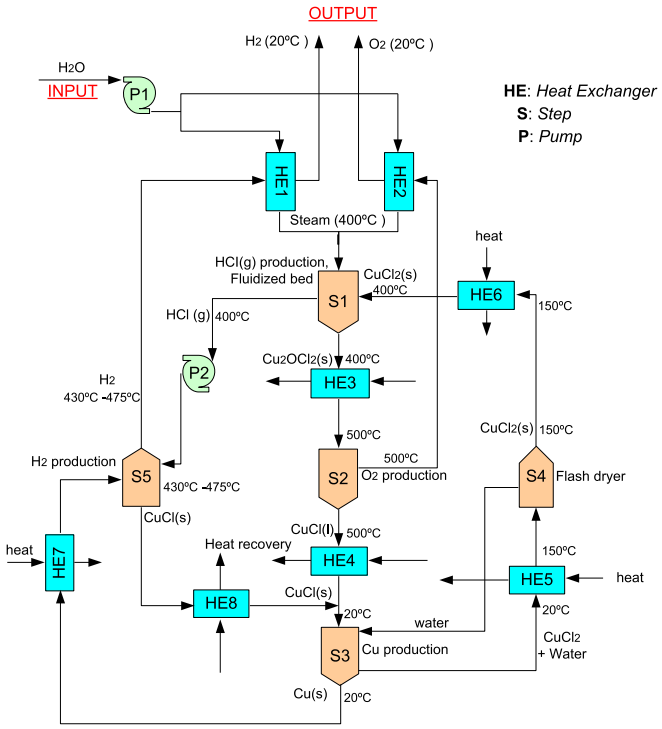

Step	Reaction	Temperature Range (°C)
S1: Hydrolysis	$2CuCl_2(s)+H_2O(g)\rightarrow CuO{*}CuCl_2(s)+2HCl(g)$	400-450
S2: O_2 Production	$CuO{*}CuCl_2(s)\rightarrow 2CuCl(l)+1/2O_2(g)$	500-550
S3: Electrolyzer	$4CuCl(s)+H_2O\rightarrow 2CuCl_2(aq)+2Cu(s)$	20-80
S4: Dryer	$CuCl_2(aq)\rightarrow CuCl_2(s)$	80-150
S5: H_2 Production	$2Cu(s)+2HCl(g)\rightarrow 2CuCl(l)+H_2(g)$	430-475

Figure 1. Conceptual flow chart of the five-step Cu–Cl cycle with associated reactions.

$$CuO{\cdot}CuCl_2(s)\rightarrow 2CuCl(l)+1/2O_2(g) \quad (2)$$

Liquid copper monochloride is solidified on being cooled to 20°C, after which it enters the copper production step (S3) with the solid copper monochloride from the hydrogen production step. In the electrolysis step, solid copper monochloride and water react endothermically at 20°C as follows:

$$4CuCl(s)+H_2O(l)\rightarrow 2CuCl_2(aq)+2Cu(s) \quad (3)$$

Here, water acts as a catalyst in this reaction and does not react. This reaction involves electrolysis and thus uses electricity, which can makes it expensive depending on the price of electricity. Solid copper and a copper chloride-water solution result. The solution (a mixture of copper chloride and water) is transferred to the dryer (S4), and the solid copper enters the hydrogen production step after being heated. The following physical reaction takes place in the dryer:

$$CuCl_2(aq)\rightarrow CuCl_2(s)+H_2O(l) \quad (4)$$

In the hydrogen production step (S5), hydrochloric gas and copper enter, and are converted to gaseous hydrogen (H_2) and solid copper monochloride (CuCl), at 450°C based on the following reaction:

$$2Cu(s)+2HCl(g)\rightarrow 2CuCl(l)+H_2(g) \quad (5)$$

3. PROCESS SIMULATION

Process simulation is used in this study, and Aspen Plus is the selected simulator. Aspen Plus [18] is a process simulator used mainly by the chemical process industry. It predicts the behavior of chemical reactions using mass and energy balances, equilibrium relationships, and rate correlations. It can also determine operating conditions; equipment sizes; and stream flow rates, compositions, and properties.

Flowsheet simulators rely on two main approaches: sequential modular and equation oriented. Aspen Plus is a sequential modular simulation program, in which a sequence is followed for each unit operation block. In contrast, Aspen Custom Modeler (previously called SPEEDUP) is equation oriented, in which equations solved simultaneously. Aspen Dynamics (previously called DynaPLUS) uses a combination of sequential modular and equation oriented approaches, by employing the Aspen Plus sequential modular for steady

state simulation and the Aspen Custom Modeler equation oriented approach for dynamic simulation.

In this article, we focus on the simulation of a nuclear-based hydrogen production process using the copper–chlorine thermochemical cycle, which is under development by University of Ontario Institute of Technology and others, to improve the understanding of the cycle and enable scale-up to facilitate development. Aspen Plus reduces plant design time, in part by allowing configurations for new designs and retrofits to be studied. The code assists in determining optimal parameter values and operating conditions, while accommodating system constraints and assessing flow compositions and conditions. In a simulation, each block represents a unit operation model (e.g., reactor, heat exchanger, pressure changer, mixer/splitter, and separator) or a user-defined model. The unit operating models perform functions based on inputs, thermodynamic models, and operating conditions.

The following steps are required for a successful simulation, using Aspen Plus or other simulators [19]:

- Select operation models for the simulation, incorporate them into a flowsheet.
- Join the unit operations with streams and identify material and energy streams (inputs and outputs).
- Specify the global setup, including units of measurement, run type, input, mode, and flow conditions.
- Specify all components involved in the process, using the simulator's database as well as non-database components.
- Specify thermodynamic models for all unit blocks to represent the physical properties of the components and mixtures.
- Specify flow rates and thermodynamic conditions of all feed streams.
- Specify the operating conditions of all unit operations.
- Perform the simulation, as well as related actions such as model and sensitivity analyses.

Two levels of modeling are utilized: component and system. The present study mainly involves two stages. First, detailed modeling of individual components of the Cu–Cl cycle is performed, using data from the literature to ensure use of the most reliable and suitable models for the main components in the cycle [1–17]. Second, a thermal model of the overall cycle is developed, accounting for energy. The two models are then coupled. Following this approach, the five-step Cu–Cl cycle is designed and analyzed. Then, thermodynamic analyses are used to determine energy requirements for the selected configuration and losses to the environment. Some relevant performance parameters are also obtained.

The Cu–Cl cycle is simulated in three stages: (i) all reactions are assumed to go to completion in stoichiometric reactors, and a simple flowsheet is developed correspondingly; (ii) this flowsheet is enhanced by using equilibrium reactors (i.e., REquil and RGibbs) to improve the accuracy of the process reaction models, in which it is assumed the chemical reactions reach thermodynamic equilibrium at specified conditions; and (iii) a user-defined electrolyzer model is added to complete the simulation.

To the best of the authors' knowledge, no precise modeling has been reported of the electrolyzer in the Cu–Cl cycle. Because of a lack of data, the device has been modeled as a stoichiometric reactor previously, with the inlet and outlet compositions defined for the cathode and anode flows and the voltage and current density assumed for the cell. Here, we develop a more precise electrolyzer model, written in Fortran as a user-defined module. There are two types of user-defined models, namely 'User' and 'User2', which allow users to interface their own unit operation model with Aspen Plus by supplying a subroutine (written in another software, e.g., Fortran) and entering its name in the main flowsheet. 'User' operation models can have up to four inlet and four outlet material streams, one information inlet stream, and one information outlet stream. On the other hand, 'User2' operation model has no limit on the number of inlet or outlet streams.

During simulation of the Cu–Cl cycles, thermodynamic data for the relevant chemical species are obtained from the literature and included in the physical property database of Aspen Plus (Table I). The values are compared with data from such sources as HSC Chemistry software [20] to ensure reliability. In some instances, the thermodynamic database in Aspen Plus is modified to improve accuracy (e.g., input values for the enthalpy of formation, the free energy of formation, and the heat capacity as a function of temperature for $CuO \cdot CuCl_2$). As data of $CuO \cdot CuCl_2$ are not available, these values are obtained via an experimental method for its synthesis [1,2]. The enthalpy of formation at 25°C was determined to be 380 ± 3 kJ/mol by two experimental methods, which is consistent with the data reported in the literature [19–22]. The heat capacity is measured over three temperature ranges: 4–64, 64–360, and 298–700 K, which are used to find the associated entropies. The free energy of formation is developed using the experimental enthalpy of formation and entropy values. As CuCl undergoes solid-solid and solid–liquid transitions, the specific enthalpy and Gibbs energy of formation of CuCl(s) at standard temperature (298.15 K) are determined, yielding respective values of −37.0 and −120.0 kJ/mol. The Gibbs energy of formation of CuCl(s) is obtained by subtracting from the enthalpy of formation of CuCl at 298.15 K, the product of the absolute temperature 298.15 K and the

Table I. Thermodynamic data used in the Aspen Plus database.

Compound	DHSFRM (kJ/mol)	DGSFRM (kJ/mol)
$CuCl_2$ (s)	−217.4	−173.6
CuO (s)	−162.0	−129.4
CuCl (s)	−137.0	−120.0
Cu (s)	0	0
$CuO \cdot CuCl_2$ (s)	−381.3	−310.45

DHSFRM: Enthalpy of formation at 298.15 K and 1 bar.
DGSFRM: Gibbs free energy of formation at 298.15 K and 1 bar.
Source: [21].

Int. J. Energy Res. 2014; **38**:1391–1402 © 2014 John Wiley & Sons, Ltd.
DOI: 10.1002/er

entropy of formation of CuCl at 298.15 K. The heats of reaction at the specified conditions are determined by the reactor models (with exothermic heat flows denoted by a negative sign).

The main chemical reactions in the five-step Cu–Cl cycle are listed in Figure 1, and an Aspen Plus flowsheet of the Cu–Cl cycle is developed (Figure 2) on the basis of these reactions. This simulation is one of the first closed-loop simulations of the Cu–Cl cycle. Hydrolysis occurs at 400°C in reactor block S1 in Figure 2, based on the equation listed in Figure 1. The products of S1 enter block SEP1 where HCl is separated from $CuO \cdot CuCl_2$. Reactor S2 represents the oxy-decomposition reaction, where oxygen gas exits and is separated via SEP2. The electrolysis step occurs in block S3, and the results are linked to the other parts of the cycle to avoid recycling problems in the electrolyzer. 'Recycling' is a common terminology used in the design of thermochemical processes. It means the reaction occurs back-and-forth, and therefore, the process recycles in the reactor continuously. To eliminate this problem, the products of the reaction are carried out to the next steps in the cycle before the reverse reaction occurs.

Drying occurs in block S4; hydrogen generation is carried out in reactor S5 via the reaction of Cu and HCl, while the resultant hydrogen gas is separated in SEP3 and other products are recycled. The simulation also utilizes heaters and coolers to exchange heat and allow effective heat supply and recovery throughout the cycle, mixers and splitters to combine and split the streams, respectively, and pumps to move fluids and supply the required water.

The corresponding heat requirements, recovered heat, work requirements, and other data for the processes at various transfer points are shown in Table II, per unit mol of hydrogen produced. With these data, energy balances and efficiencies are evaluated for the cycle. The total heat transfers are found to be 501.9 kJ input for the endothermic processes and 210.8 kJ output for the exothermic processes. The output heat is recovered heat within the cycle to supply part of the requirements for the endothermic processes, resulting in a net heat requirement of 291.1 kJ. The electrical energy required in the electrolysis unit and auxiliary devices (e.g., operate pumps and compressors) in other processes is also calculated. Assuming an energy efficiency of 40% for converting heat to electricity, the value of 97.6 kJ work in Table II necessitates an input of 244 kJ heat.

The overall energy efficiency of the Cu–Cl cycle is determined as follows, based on the ratio of product output energy (as measured by the lower heating value for hydrogen LHV_{H_2}, i.e., is 240 kJ/mol H_2) to input energy:

$$\eta_e = \frac{LHV_{H_2}}{Q_{net} + W} \tag{6}$$

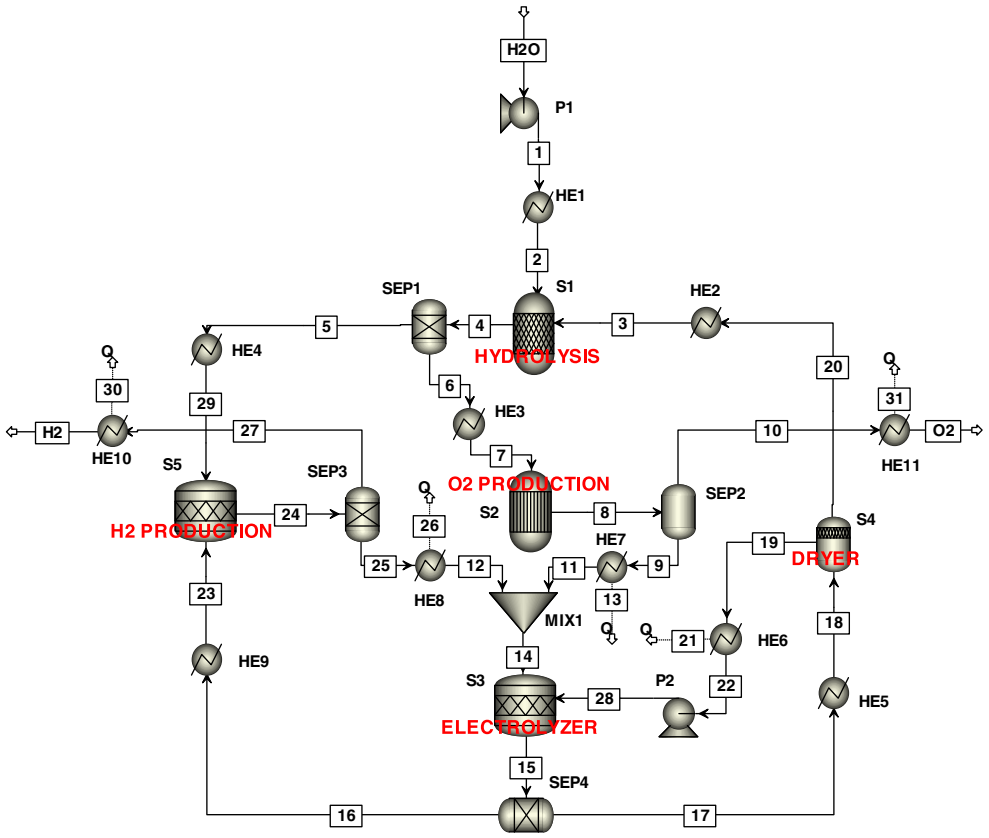

Figure 2. Simplified Aspen Plus process flowsheet of the five-step Cu–Cl cycle.

Table II. Energy results of Aspen Plus process simulation of the five-step Cu–Cl cycle.

Block	Description	Process	ΔH Endothermic (kJ/mol H_2)	ΔH Exothermic (kJ/mol H_2)	W (kJ/mol H_2)
S1	Step 1	$2CuCl_2(s) + H_2O(g) \xrightarrow{400°C} CuO \cdot CuCl_2(s) + 2HCl(g)$	120.2	—	—
S2	Step 2	$CuO \cdot CuCl_2(s) \xrightarrow{500°C} 2CuCl(l) + 1/2O_2(g)$	125.5	—	—
S3	Step 3	$4CuCl(s) + H_2O(l) \xrightarrow{25°C} 2CuCl_2(aq) + 2Cu(s)$	—	—	53.2
S4	Step 4	$CuCl_2(aq) \xrightarrow{80°C} CuCl_2(s)$	—	—	33.2
S5	Step 5	$2Cu(s) + 2HCl(g) \xrightarrow{450°C} 2CuCl(l) + H_2(g)$	—	−41.6	—
HE1	Heat exchanger	H_2O (25°C) ⟶ H_2O (400°C)	80	—	—
HE2	Heat exchanger	$CuCl_2$ (80°C) ⟶ $CuCl_2$ (400°C)	61.3	—	—
HE3	Heat exchanger	$CuO \cdot CuCl_2$ (400°C) ⟶ $CuO \cdot CuCl_2$ (500°C)	20.8	—	—
HE4	Heat exchanger	HCl (400°C) ⟶ HCl (450°C)	4.0	—	—
HE5	Heat exchanger	$CuCl_2/H_2O$ (25°C) ⟶ $CuCl_2/H_2O$ (80°C)	57.6	—	—
HE6	Heat exchanger	H_2O (80°C) ⟶ H_2O (25°C)	—	−30	—
HE7	Heat exchanger	CuCl (500°C) ⟶ CuCl (25°C)	—	−64	—
HE8	Heat exchanger	CuCl (450°C) ⟶ CuCl (25°C)	—	−60.6	—
HE9	Heat exchanger	Cu (25°C) ⟶ Cu (450°C)	32.5	—	—
HE10	Heat exchanger	H_2 (450°C) ⟶ H_2 (25°C)	—	−9	—
HE11	Heat exchanger	O_2 (500°C) ⟶ O2 (25°C)	—	−5.6	—
SEP 1	Separator	$(CuO \cdot CuCl_2, HCl)_{mix} \xrightarrow{400°C} (CuO \cdot CuCl_2) + (HCl)$	—	—	0.87
SEP 2	Separator	$(CuCl, O_2)_{mix} \xrightarrow{500°C} (CuCl) + (O_2)$	—	—	1.2
SEP 3	Separator	$(CuCl, H_2)_{mix} \xrightarrow{450°C} (CuCl) + (H_2)$	—	—	1.8
SEP 4	Separator	$(Cu, CuCl_2(aq))_{mix} \xrightarrow{25°C} (Cu) + (CuCl_2(aq))$	—	—	2
P1	Pump	Water feed to the cycle	—	—	3
P2	Pump	Water handling within the cycle	—	—	1.93
MIX 1	Mixer	Mixing CuCl from stream 11 and 12	—	—	0.4
TOTAL			501.9	−210.8	97.6

Here, W denotes the equivalent heat to generate electrical energy required by the elecrolyzer and shaft work for other processes, and Q_{net} is the net heat utilized by the process to produce hydrogen. Consequently,

$$\eta_e = \frac{240 \text{ kJ/mol } H_2}{(291.1 \text{ kJ/mol } H_2) + (244 \text{ kJ/mol } H_2)} = 0.448$$

The thermal efficiency value given earlier is subjected to variation on the basis of the operation parameters. Associated sensitivity analysis and process optimization are given in the following section. Furthermore, detailed efficiency analyses of the cycle have been presented by authors elsewhere [22,23].

4. SENSITIVITY ANALYSIS AND PROCESS OPTIMIZATION

In Table II, all analyses are carried out per one mole of hydrogen produced. Thus, all five reactions in the cycle are balanced for one mole of hydrogen produced. However, variation of reaction yields with operation parameters is given in the sensitivity analysis.

Sensitivity analyses are performed for the process flowsheet in Figure 2 with the data in Table II, by assessing each of the main steps in the five-step Cu–Cl cycle to determine how it varies as operating and design variables are modified. Typically, the effect on process parameters is determined as one or more flowsheet variables are varied. The trends identified likely can assist in optimization activities.

4.1. Hydrolysis reactor

In the hydrolysis reactor in Figure 3, where hydrolysis occurs in block S1 in Figure 2 and represents Step 1 of the five-step Cu–Cl cycle, pressurized, hot $CuCl_2$ is sprayed into a superheated vapor at 400°C, forming a free jet that undergoes significant heat and mass transfer. Superheated vapor and the $CuCl_2$ react, yielding $CuO \cdot CuCl_2$ and HCl, according to the following reaction: $2CuCl_2(s) + H_2O(g) \rightarrow CuO \cdot CuCl_2(s) + 2HCl(g)$.

We examine the sensitivity of the hydrolysis reaction (Figures 4 and 5), utilizing the modified thermodynamic database. The hydrolysis reactor typically aims to maximize the yield of $CuO \cdot CuCl_2$ while avoiding side-product formation. Various ratios of the input steam and $CuCl_2$ are considered. The effect of reaction temperature on $CuO \cdot CuCl_2$ yield is illustrated in Figure 4 for $H_2O/CuCl_2$ ratios of 10, 15, and 20. The $CuO \cdot CuCl_2$ yield is observed to increase with reaction temperature to 400°C, above which it decreases. Further, excess steam (relative to the stoichiometric requirements) is needed to achieve high yields, for

Int. J. Energy Res. 2014; **38**:1391–1402 © 2014 John Wiley & Sons, Ltd.
DOI: 10.1002/er

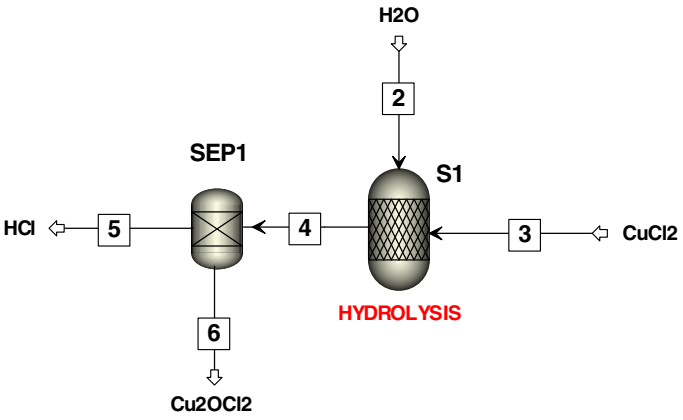

Figure 3. Hydrolysis reactor.

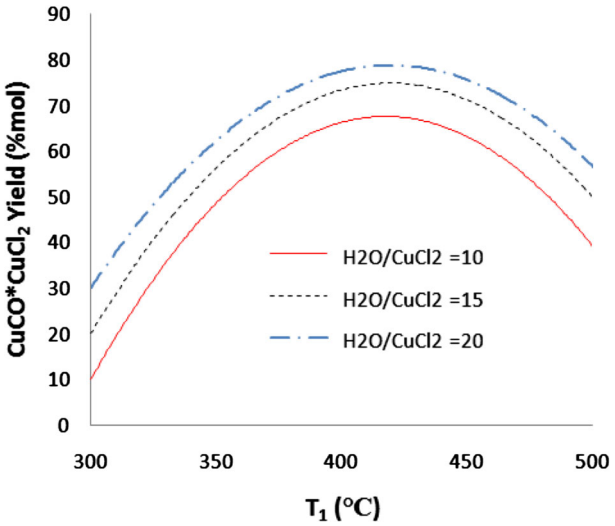

Figure 4. Effect of reaction temperature on the $CuO \cdot CuCl_2$ yield of hydrolysis process.

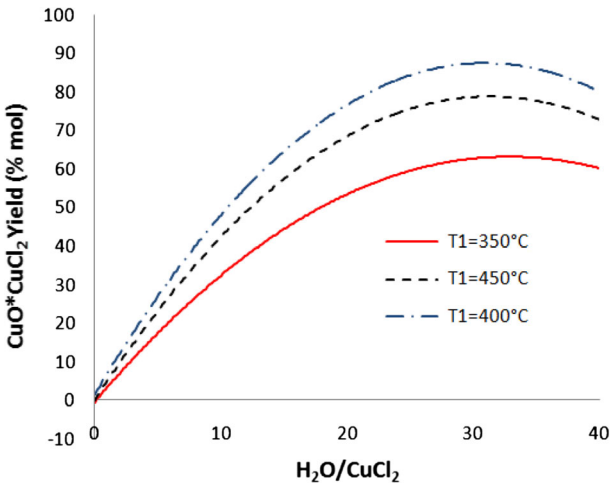

Figure 5. Effect of $H_2O/CuCl_2$ ratio on the $CuO \cdot CuCl_2$ yield of hydrolysis process at three different reaction temperature.

example, a $H_2O/CuCl_2$ ratio over 10 is needed to achieve a $CuO \cdot CuCl_2$ yield exceeding 70% at 400°C. The effect of $H_2O/CuCl_2$ ratio on the $CuO \cdot CuCl_2$ yield is illustrated in Figure 5 for reaction temperatures of 350°C, 400°C, and 450°C. $CuO \cdot CuCl_2$ yield is significantly affected by $H_2O/CuCl_2$ ratio until it reaches 30, above which the effect decrease until it becomes nearly constant for a ratio of 40. At that point, the $CuO \cdot CuCl_2$ yield concentration peaks at 80% mol.

The variation with reaction temperature of the reaction heat of HCl production is illustrated in Figure 6 for percentage yield (y_p) values of 100% and 80%. As reaction temperature increases, the reaction heat for HCl production decreases nearly linearly, in part linked to the endothermic reaction occurring in the fluidized bed.

4.2. Oxy-decomposition reactor

During oxygen production in a molten salt reactor (oxy-decomposition reactor), Step 2 in Figure 2 and shown in Figure 7, the following reaction occurs at 480–530°C with an endothermic reaction heat load of 125.5 kJ/mol: $CuO \cdot CuCl_2(s) \rightarrow 2CuCl(l) + 1/2O_2(g)$. The solid product of hydrolysis enters the oxy-decomposition reactor, where $CuO \cdot CuCl_2$ is heated to 500ºC and decomposes to oxygen gas and molten CuCl, and the products are separated in the gas–liquid separator (block SEP2 in Figure 7). The viscosity of molten CuCl at 430°C is 2.6 cp, and its melting and boiling points, respectively, are 430°C and 1490°C. CuCl has a density of 3.692 g/cm^3 when molten at 430°C and 4.140 g/cm when solid at 25°C. Because the density of the $CuO \cdot CuCl_2$ reactant is 4.853 g/cm^3, the volume expansion coefficient, assuming oxygen is removed immediately from the reactor, from solid reactant $CuO \cdot CuCl_2(s)$ to molten product 2CuCl is 1.22.

The dependence of reaction temperature on oxygen production during oxy-decomposition is illustrated in Figure 8, where it is observed that oxygen generation commences at a temperature as low as 350°C and increases to a peak at approximately 450°C, for reaction efficiency (η) values of 80% and 100% (complete reaction). The oxygen yield is nearly constant as temperature increases above 450°C. Traces of side products (i.e., chlorine gas) are observed

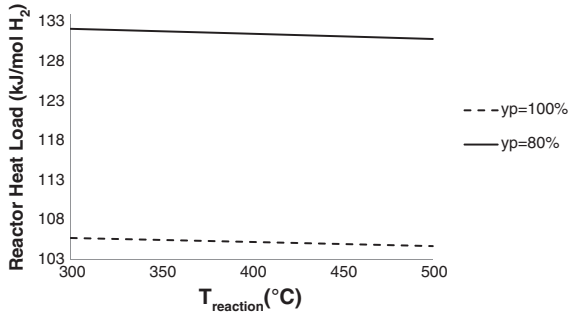

Figure 6. Effect of reaction temperature on the reaction heat of hydrolysis step.

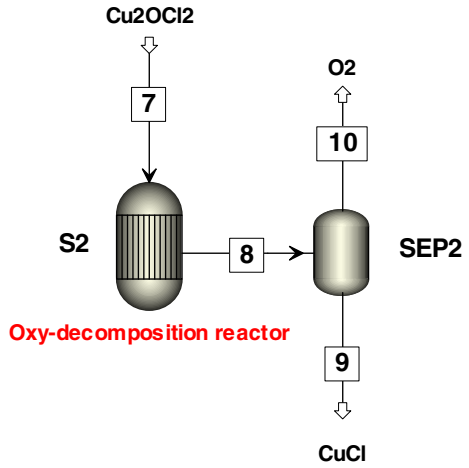

Figure 7. Oxygen production process.

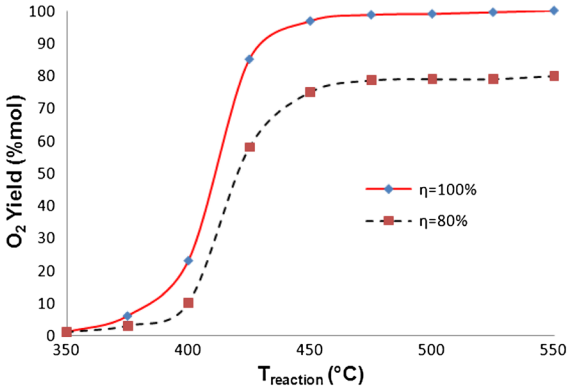

Figure 8. Effect of reaction temperature on the oxygen yield at two different reaction efficiencies.

for incomplete reaction cases, with the side-product generation increasing with temperature to a peak at 450°C and thereafter declining until the reactor temperature reaches 550°C and the generation rate of side-products becomes negligible. Production of undesirable side products can be reduced or avoided through enhanced reactor design and operating conditions [24].

The variation of oxy-decomposition reaction heat with reaction temperature is illustrated in Figure 9, where the reaction heat for O_2 production is seen to increase as reaction temperature rises.

4.3. Electrolyzer

Heat is recovered in a direct heat exchanger from the molten CuCl stream of oxy-decomposition (Step 2) and H_2 production (Step 5). The molten CuCl is inputed to the electrolysis reactor as it cools and solidifies (Figure 10).

A conceptual design for the electrolyzer is modeled in Aspen Plus. Cl^- ions flow through an electrolyte ion exchange membrane, which causes a flow of electrons in

Int. J. Energy Res. 2014; **38**:1391–1402 © 2014 John Wiley & Sons, Ltd.
DOI: 10.1002/er

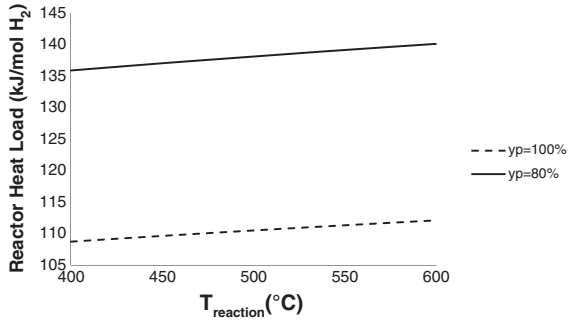

Figure 9. Effect of reaction temperature on the reaction heat of O_2 production step.

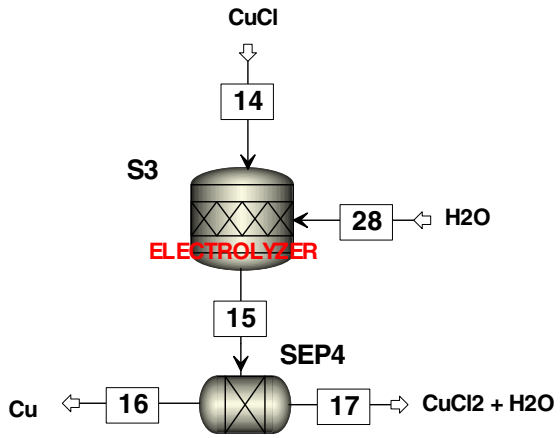

Figure 10. Electrolysis process.

the opposite direction. The crossing of ions and electrons in opposite directions results in Cu(s) and $CuCl_2$(aq) production. An electrolytic membrane, where recycled water and granulated CuCl are collected in a tank as feed for the anode, is shown in Figure 11. The solution containing dissolved CuCl passes to the electrolyzer anode and cathode, and the Cl^- ions travel across the membrane from the cathode, where Cu is produced, to the anode, where they react with CuCl to produce $CuCl_2$. The anolyte solution is then transferred to the dryer where H_2O is separated from the $CuCl_2$(s), which exits the dryer as a solid and enters the hydrolysis reactor. Aspen Plus cannot directly model this type of electrolyte ion exchange membrane because it does not contain the relevant unit operation models. But user-defined calculations performed independent of Aspen Plus, which are carried out in user-defined unit operation blocks, can be used to perform the relevant modeling for the ion exchange membranes and electrolysis process in Figure 11. The specifications of the user-defined unit block operation and its interaction with the flowsheet simulation are stipulated by the user. Here, the user-defined calculations utilize Fortran and Excel programming, and HSC Chemistry software.

The variation of reaction energy during Cu production with reaction temperature is illustrated in Figure 12, where the reaction energy is observed to decrease as reaction temperature rises.

4.4. Flash dryer

During drying (expressed as $2CuCl_2(aq) \rightarrow 2CuCl_2(s)$ and denoted Step 4 in Figures 1 and 13), aqueous $CuCl_2$ exiting from the electrolysis cell is dried to solid $CuCl_2$(s), which is required for hydrolysis for the production of copper

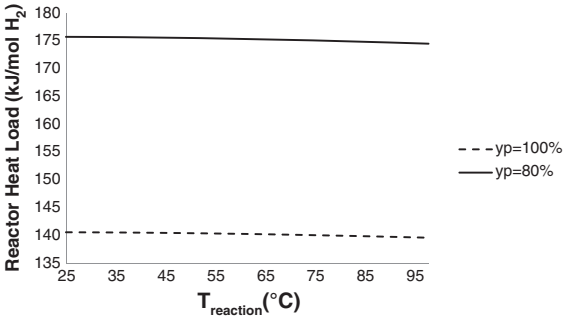

Figure 12. Effect of reaction temperature on the reaction heat of electrolysis step.

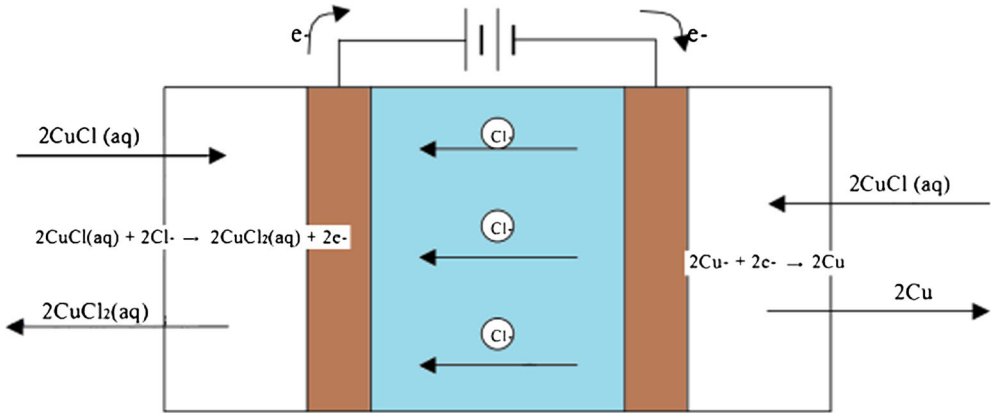

Figure 11. Electrolysis cell in the electrolyzer.

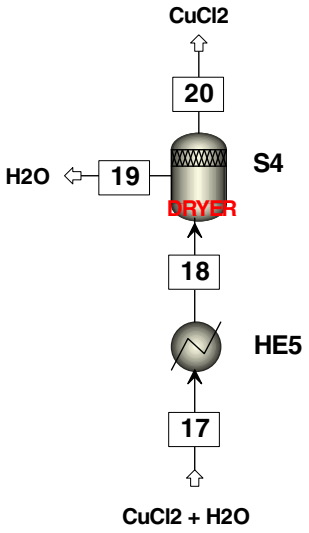

Figure 13. Flash dryer.

oxychloride ($CuO \cdot CuCl_2$) and HCl gas. Although greater in quantity than for other steps in the cycle, the heat for drying is required at a lower temperature (below 100°C) or quality. Obtaining this heat as waste or recovered heat can raise the overall cycle efficiency. A commercial spray dryer can be used, as spray drying is an efficient method of water removal when the liquid is atomized into adequately small droplets, due to the relatively large surface area available for heat and mass transfer [25].

The effect on the dryer heat load of varying the dryer temperature T_{dryer} and inlet temperature of CuC_2/H_2O mixture, respectively, are illustrated in Figure 14 and 15. The heat to evaporate water varies in direct proportion to the evaporator temperature but decreases almost linearly as inlet temperature increases. The evaporator inlet temperature is determined by the copper production process, where the reaction temperature is 25–80°C.

4.5. H_2 production reactor

Hydrogen production (Figure 16) occurs exothermically according to $2Cu(s) + 2HCl(g) \rightarrow 2CuCl(l) + H_2(g)$, with a

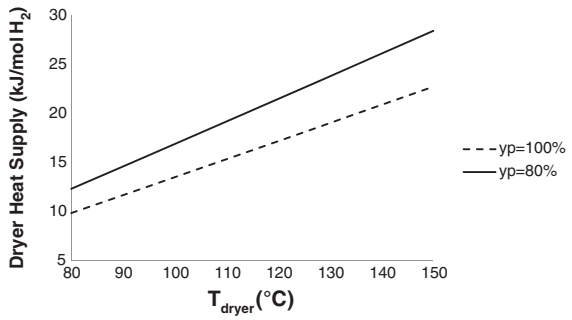

Figure 14. Effect of drying temperature on the dryer inlet heat.

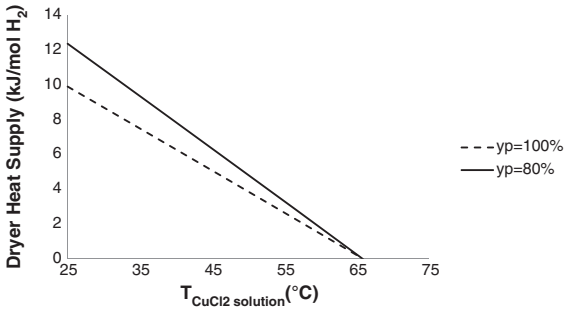

Figure 15. Effect of inlet copper chloride solution temperature on the dryer heat input.

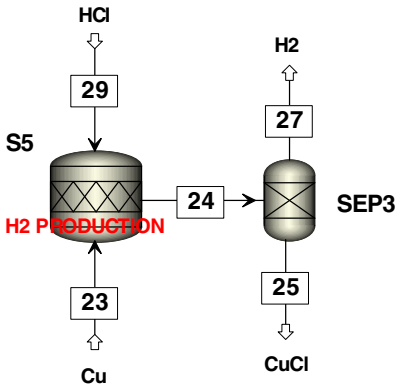

Figure 16. Hydrogen production reactor.

reaction heat of −41.6 kJ/mol H_2 at 450°C. The molar masses of reactants and products follow: $H_2 = 2$, Cu = 63.45, CuCl = 98.99, and HCl = 36.46. The boiling point of CuCl is 1490°C and the melting point is 430°C, at which the density in the liquid phase is 3.692 g/cm^3 and the viscosity is 2.6 cp [24].

The variation of the reaction heat during the exothermic H_2 production step with reaction temperature is shown in Figure 17, where it is observed that the reaction heat for H_2 production decreases nearly linearly as the reaction temperature increases.

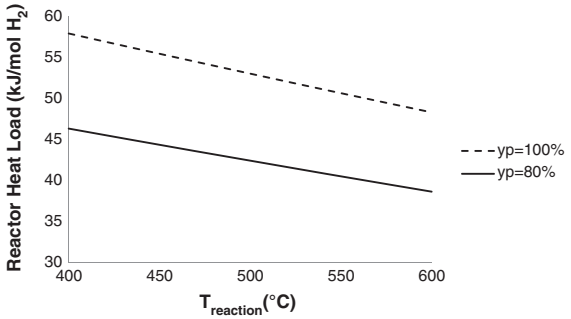

Figure 17. Effect of reaction temperature on the reaction heat of hydrogen production step.

Int. J. Energy Res. 2014; **38**:1391–1402 © 2014 John Wiley & Sons, Ltd.
DOI: 10.1002/er

5. CONCLUSIONS

The design and simulation of the five-step Cu–Cl cycle using Aspen Plus improves understanding of the cycle and may facilitate scale-up to allow construction in the future. The design and analysis techniques used require a minimum of data, and provide help in improving and optimizing complex thermal systems. These analyses are useful for evaluating the potential for improving the cycle efficiency and cost effectiveness, and assist ongoing efforts [1–28] to understand better thermodynamic losses in the cycle and to improve efficiency.

Some important observations that can be drawn from the study follow:

- The reaction heat for many chemical reaction steps varies with reaction temperature.
- A maximum is observed at about 400°C in the variation $CuO \cdot CuCl_2$ yield with reaction temperature.
- Excess steam is needed to achieve high $CuO \cdot CuCl_2$ yields, and $CuO \cdot CuCl_2$ yield is affected by $H_2O/CuCl_2$ ratio until a ratio of around 30, for which the $CuO \cdot CuCl_2$ yield concentration peaks at 80% mol.
- Oxygen generation commences at about 350°C and increases to a peak at approximately 450°C.
- The efficiency of the Cu–Cl cycle is 44% based on the lower heating value of hydrogen.
- Although greater in quantity than for other steps in the cycle, the heat for drying is required at a low temperature (below 100°C), providing opportunities for efficiency improvement via low quality thermal energy supplies.

ACKNOWLEDGEMENTS

The authors acknowledge gratefully the financial support provided by the Ontario Research Excellence Fund and Atomic Energy of Canada Limited.

REFERENCES

1. Lewis MA, Ferrandon MS, Tatterson DF, Mathias P. Evaluation of alternative thermochemical cycles—part III further development of the Cu-Cl cycle. *International Journal of Hydrogen Energy* 2009; **34**:4136–45.
2. Lewis MA, Masin JG. The evaluation of alternative thermochemical cycles—part II: the down-selection process. *International Journal of Hydrogen Energy* 2009; **34**:4125–35.
3. Naterer GF, Suppiah S, Lewis M, Gabriel K, Dincer I, Rosen MA, *et al*. Recent Canadian advances in nuclear-based hydrogen production and the thermochemical Cu-Cl cycle. *International Journal of Hydrogen Energy* 2009; **34**:2901–17.
4. Al-Dabbagh AW, Lu L. Design and reliability assessment of control systems for a nuclear-based hydrogen production plant with copper–chlorine thermochemical cycle. *International Journal of Hydrogen Energy* 2010; **35**:966–77.
5. Daggupati VN, Naterer GF, Gabriel KS, Gravelsins RJ, Wang ZL. Equilibrium conversion in Cu–Cl cycle multiphase processes of hydrogen production. *Thermochimica Acta* 2009; **496**:117–23.
6. Daggupati VN, Naterer GF, Gabriel KS. Diffusion of gaseous products through a particle surface layer in a fluidized bed reactor. *International Journal of Heat and Mass Transfer* 2010; **53**:2449–58.
7. Daggupati VN, Naterer GF, Gabriel KS, Gravelsins RJ, Wang ZL. Solid particle decomposition and hydrolysis reaction kinetics in Cu-Cl thermochemical hydrogen production. *International Journal of Hydrogen Energy* 2010; **35**:4877–82.
8. Zamfirescu C, Dincer I, Naterer GF. Thermophysical properties of copper compounds in copper–chlorine thermochemical water splitting cycles. *International Journal of Hydrogen Energy* 2010; **35**:4839–52.
9. Zamfirescu C, Naterer GF, Dincer I. Kinetics study of the copper/hydrochloric acid reaction for thermochemical hydrogen production. *International Journal of Hydrogen Energy* 2010; **35**:4853–60.
10. Rosen MA, Naterer GF, Chukwu CC, Sadhankar R, Suppiah S. Nuclear-based hydrogen production with a thermochemical copper-chlorine cycle and supercritical water reactor: equipment scale-up and process simulation. *International Journal of Energy Research* 2012; **36**:456–65.
11. Wang ZL, Naterer GF, Gabriel KS. Multiphase reactor scale-up for Cu–Cl thermochemical hydrogen production. *International Journal of Hydrogen Energy* 2008; **33**:6934–46.
12. Jaber O, Naterer GF, Dincer I. Heat recovery from molten CuCl in the Cu-Cl cycle of hydrogen production. *International Journal of Hydrogen Energy* 2010; **35**:6140–51.
13. Ferrandon MS, Lewis MA, Alvarez F, Shafirovich E. Hydrolysis of $CuCl_2$ in the Cu-Cl thermochemical cycle for hydrogen production: experimental studies using a spray reactor with an ultrasonic atomizer. *International Journal of Hydrogen Energy* 2010; **35**:1895–904.
14. Ferrandon MS, Lewis MA, Tatterson DF, Doizi D, Croizé L, Dauvois V, *et al*. Hydrogen production by the Cu-Cl thermochemical cycle: investigation of the key step of hydrolysing $CuCl_2$ to Cu_2OCl_2 and HCl using a spray reactor. *International Journal of Hydrogen Energy* 2010; **35**:992–1000.
15. Ranganathan S, Easton EB. Ceramic carbon electrode-based anodes for use in the Cu-Cl thermochemical

cycle. *International Journal of Hydrogen Energy* 2010; **35**:4871–6.
16. Ranganathan S, Easton EB. High performance ceramic carbon electrode-based anodes for use in the Cu–Cl thermochemical cycle for hydrogen production. *International Journal of Hydrogen Energy* 2010; **35**:1001–7.
17. Wang ZL, Naterer GF, Gabriel KS, Gravelsins R, Daggupati VN. Comparison of sulfur-iodine and copper–chlorine thermochemical hydrogen production cycles. *International Journal of Hydrogen Energy* 2010; **35**:4820–30.
18. Aspen Technology Inc., Cambridge, MA, 2010.
19. Chukwu C. Process analysis and aspen plus simulation of nuclear-based hydrogen production with a copper-chlorine cycle. MASc Thesis in Mechanical Engineering, UOIT. Oshawa, 2008.
20. Outotec Research Oy, Antti Roine, HSC Chemistry 7, Espoo, Finland, 2010.
21. Ferrandon MS, Lewis MA, Tatterson DF, Nankanic RV, Kumarc M, Wedgewood LE, *et al.* The hybrid Cu–Cl thermochemical cycle. I. Conceptual process design and H2A cost analysis. II. Limiting the formation of CuCl during hydrolysis. NHA Annual Hydrogen Conference, Sacramento Convention Center, CA; March 30-April 3, 2008.
22. Orhan MF, Dincer I, Rosen MA. Efficiency analysis of a hybrid copper–chlorine (Cu–Cl) cycle for nuclear-based hydrogen production. *Chemical Engineering Journal* 2009; **155**:132–37.
23. Orhan MF, Dincer I, Rosen MA. Efficiency comparison of various design schemes for copper–chlorine (Cu–Cl) hydrogen production processes using Aspen Plus software. *Energy Conversion and Management* 2012; **63**:70–86.
24. Naterer GF, Suppiah S, Stolberg L, Lewis M, Wang Z, Daggupati V, *et al.* Canada's program on nuclear hydrogen production and the thermochemical Cu–Cl cycle. *International Journal of Hydrogen Energy* 2010; **35**:10905–26.
25. Orhan MF, Dincer I, Rosen MA. Design of systems for hydrogen production based on the Cu–Cl thermochemical water decomposition cycle: configurations and performance. *International Journal of Hydrogen Energy* 2011; **36**:11309–20.
26. Orhan MF, Dincer I, Rosen MA, Kanoglu M. Integrated hydrogen production options based on renewable and nuclear energy sources. *Renewable and Sustainable Energy Reviews* 2012; **16**:6059–82.
27. Orhan MF, Dincer I, Rosen MA. Design and simulation of a UOIT copper–chlorine cycle for hydrogen production. *International Journal of Energy Research* 2013; **37**:1160–74.
28. Orhan MF, Dincer I, Rosen MA. Investigation of an integrated hydrogen production system based on nuclear and renewable energy sources: a new approach for sustainable hydrogen production via copper–chlorine thermochemical cycles. *International Journal of Energy Research* 2012; **36**:1388–94.